Radio Science, Volume 35, Number 6, Pages 1437–1444, November–December 2000

Ionospheric *E* region remote sensing with ELF radio atmospherics

Steven A. Cummer

Electrical and Computer Engineering Department, Duke University, Durham, North Carolina

Umran S. Inan

Space, Telecommunications and Radioscience Laboratory, Stanford University, Stanford, California

Abstract. Radio remote sensing of the ionospheric *E* region can be difficult, particularly in the nighttime *E* region valley which lies between two regions of higher electron density. We show that extremely low frequency (ELF) electromagnetic waves launched from below penetrate this region because of their low attenuation and can be reflected from both the *D* region and the top of the *E* region valley. This double reflection, also caused by sporadic *E* layers, produces a measurable effect on the subionospheric propagation of ELF waves, which we demonstrate with numerical Earth-ionosphere waveguide simulations. This sensitivity opens the possibility of remotely sensing the *E* region and detecting sporadic *E* layers with broadband ELF propagation measurements using lightning discharges as the source. From nighttime observations of ELF lightning radiation over the same propagation path on different days, we extract *E* region electron density profiles that show significant variability not only from day to day but over the course of a single night. This technique is inherently a path-integrated measurement, enabling tomographic large-scale ionospheric remote sensing with multiple sources and receivers.

1. Introduction

Because of its relative inaccessibility the lower ionosphere, consisting of the *D* and *E* regions, is among the least studied regions of the Earth's atmosphere. The altitudes involved (~70–140 km) are too high for balloons and too low for most satellites, making in situ measurements difficult. Radio sounding does not always work because the electron densities in this region are often too low to reflect radio waves with ionosonde and incoherent scatter radar, particularly at night. Rocket experiments [e.g., *Mechtly et al.*, 1967] have measured this region but only in limited spatial and temporal extents.

Very low frequency (VLF, 3–30 kHz) and extremely low frequency (ELF, 3–3000 Hz) electromagnetic waves are strongly reflected by the *D* and *E* regions and can therefore be used for radio sounding of these altitudes [*Sechrist*, 1974]. However, at ELF and VLF, transmitters are extremely large and expensive because of the long wavelengths involved [*Watt*, 1967], making such sounding difficult in practice. Nevertheless, man-made VLF transmitters have been used very successfully to remotely sense perturbations in this region of the ionosphere [e.g., *Johnson et al.*, 1999].

Lightning is a powerful broadband source of VLF and ELF energy and can be used as a source for sounding the lower ionosphere. *Cummer et al.* [1998] showed that broadband VLF radiation from lightning can be used to measure an assumed *D* region electron density profile with an altitude and scale height accuracy of a few hundred meters. In this work, we show that ELF radiation from lightning is partially reflected from *E* region altitudes and that subionospheric ELF propagation measurements from lightning can be used to sound the *E* region, including the *E* region valley, which is difficult to probe from the ground. We also show theoretically that subionospheric ELF propagation is very sensitive to the presence of sporadic *E* layers (E_s). The method we describe measures path-integrated electron density profiles and therefore, with multiple sources (i.e., lightning lo-

Paper number 2000RS002335.
0048-6604/00/2000RS002335$11.00

cations) and receivers, can be used to tomographically measure three-dimensional ionospheric structure on large spatial scales.

Previous theoretical studies have demonstrated the sensitivity of ELF propagation to E region electron densities. *Pappert and Moler* [1974, 1978] showed with full wave model calculations that E_s and sharp electron density gradients around 250 km altitude produce significant attenuation maxima below 100 Hz. *Barr* [1977] showed, again with full wave calculations, that E_s drastically affects ELF attenuation rates by generating a series of resonances from 10 to 1000 Hz and that the E_s characteristics affect the frequencies and depth of these resonances. In this paper, we show that the nighttime E region valley generates weaker but measurable ELF resonances that depend strongly on the details of the electron density profile.

ELF propagation experiments have been performed with man-made, single-frequency transmitters [*Bannister*, 1975] and with radio atmospherics [*Hughes and Gellenberger*, 1974]. These authors observed significant variability in ELF attenuation rates, but the limited frequency ranges and spectral smoothing from temporal averaging tended to obscure the resonances which enable the remote sensing described in this work.

2. ELF Penetration Into the E Region

The nominal reflection altitude of electromagnetic waves in the ionosphere varies with frequency, with lower frequencies usually reflected by lower electron densities and therefore at lower altitudes. In the F region, where electron collisions are infrequent enough to be relatively unimportant, vertically incident ordinary O and extraordinary X waves are reflected at the altitude where $f_P = f$ and $f_P^2 = f^2 - ff_B$, respectively, where f is the wave frequency, f_P is the electron plasma frequency, and f_B is the electron gyrofrequency [*Budden*, 1985, p. 357]. The O and X modes are the two characteristic waves that result from propagation in an anisotropic plasma. Each mode has its own polarization and index of refraction, and the polarization, while frequency dependent, is often circular. As the wave frequency is reduced, the O and X reflection altitudes move downward into regions where electron collisions can be significant and these reflection heights are not necessarily valid. In this regime, *Budden* [1985, p. 361] describes the reflection as occurring at a complex altitude, but it is not clear how this complex altitude relates to the real altitude below which most of the wave energy is confined. *Ratcliffe* [1959, p. 140] shows that significant ordinary mode reflection occurs under these conditions at the higher of the altitudes where $f_P^2 = ff_B$ and $f_P^2 = f\nu$ are satisfied.

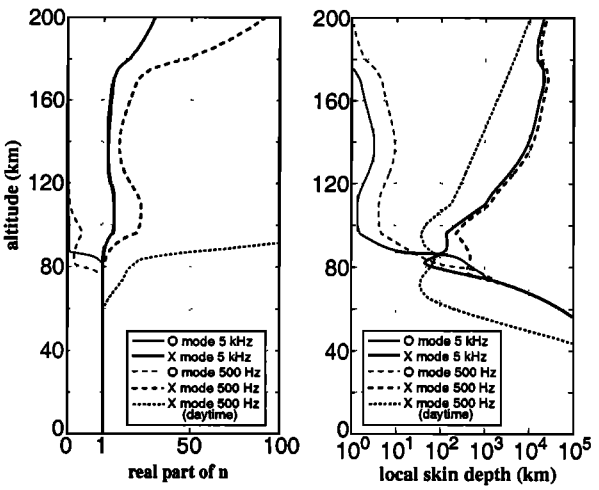

Figure 1. Index of refraction n and skin depth for vertically incident X- and O-mode waves in a model nighttime ionosphere at 5 kHz and 500 Hz and for the 500 Hz X mode in a daytime ionosphere. The lower losses and sharper n gradient at 180 km altitude for the nighttime X mode at 500 Hz can produce a significant E-F region reflection.

The extraordinary mode is only weakly reflected except by extremely sharp ionospheric gradients and therefore penetrates more deeply into the ionosphere. It is this mode that can be reflected by E or F region gradients substantially above the O-mode reflection altitude if the frequency is sufficiently low. Figure 1 shows the O- and X-mode indexes of refraction n at 5 kHz and 500 Hz for vertical incidence as a function of altitude in a model nighttime ionosphere and the X-mode n at 500 Hz for a daytime ionosphere. Expressions for the index of refraction in a cold plasma are given by *Budden* [1985, p. 74]. The left panel of Figure 1 shows the real part of n on a nonlinear scale to show both modes, while the right panel shows the local skin depth (or amplitude e-folding depth) and reflects the losses of the waves. At night, n_O drops around 80 km for both frequencies, and above this altitude the losses are very high (skin depths of 10 km and less). Thus the O mode is only reflected near 80 km. In contrast, the nighttime n_X changes gradually, the losses are significantly lower, and therefore the X mode significantly penetrates the nighttime ionosphere. However, at 500 Hz the losses are much lower between 70 and 120 km altitude, and the gradient in n at 180 km is much sharper than at 5 kHz. Thus the X mode undergoes some reflection in the nighttime E-F region, and the combination of gradients and losses makes this reflection stronger

at lower frequencies. During the day, however, X-mode losses are larger at 500 Hz, the sharp n gradient moves down to 90 km altitude, and the X mode does not penetrate to the E-F region. It is the nighttime X mode E-F region reflection that affects subionospheric ELF propagation and forms the basis for the remote sensing technique described in this work.

3. E Region Effect on Subionospheric ELF Propagation

Because of the secondary ELF reflections from the E region, subionospheric ELF propagation depends on the electron density at these altitudes. This dependence can be demonstrated numerically with the Long Wave Propagation Code (LWPC) [*Pappert and Ferguson*, 1986], which is commonly used for VLF calculations but is also valid and has been used at ELF [*Pappert and Moler*, 1974]. Figure 2 shows two midlatitude electron density profiles from the 1995 international reference ionosphere [*Bilitza*, 1997] and a third with a model E_s layer. Of the two non-E_s profiles, one contains a significant E region valley depletion, and the other does not. All of the profiles are identical below 90 km. The ionospheric magnetic field in all the simulations is typical of east-to-west propagation over the continental United States. Ions play a significant role in subionospheric ELF propagation [*Pappert and Moler*, 1974], and we assume throughout this work that the positive ion density $N_i^+ = N_e$ where $N_e > 10^2$ and that $N_i^+ = 10^2$ where $N_e < 10^2$, with negative ions

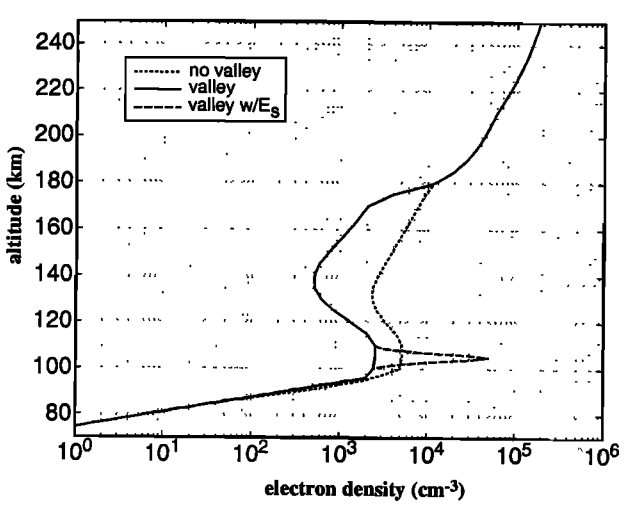

Figure 2. Three nighttime electron density profiles with different E region characteristics and one with an E_s layer. The profiles are identical below 90 km.

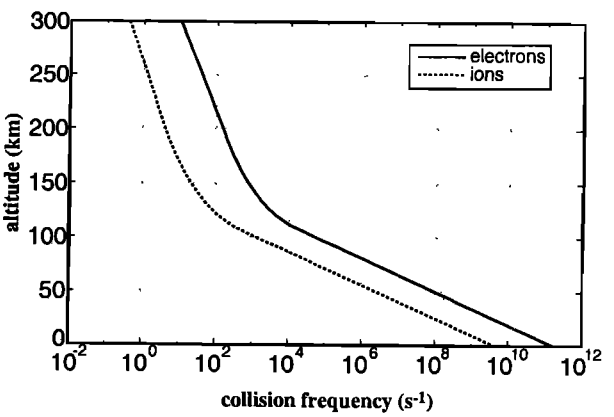

Figure 3. Electron and ion collision frequency profiles used in the simulations throughout this paper.

present as required for charge neutrality. The electron and ion collision frequency profiles used throughout this work are a concatenation of D region profiles of *Morfitt and Shellman* [1976] and E and F region values of *Rishbeth and Garriott* [1969, p. 131] and are plotted in Figure 3.

In the Earth-ionosphere waveguide the unconfined O and X plasma waves combine into waveguide modes that contain both waves. The number of propagating modes depends on the frequency relative to the waveguide cutoff frequencies. We use the LWPC to calculate the waveguide propagation constants (phase velocity and attenuation) of the single quasi-transverse electromagnetic (QTEM) mode that propagates at ELF (the other modes are evanescent). Figure 4 shows these quantities as a function of frequency for the three ionospheres shown in Figure 2 with the collision frequency profiles in Figure 3. The significant variations with ionosphere demonstrate the importance of the E region for ELF propagation.

This specific E_s layer creates a strong attenuation maximum at 400 Hz. The depth and frequency of this maximum depend on the altitude and maximum N_e of the E_s layer [*Barr*, 1977]. However, even the E region valley profile without E_s produces distinct attenuation maxima at approximately 250, 520, and 750 Hz and attenuation minima at 400, 630, and 900 Hz. In both cases, a resonance phenomenon appears to be responsible for the variations, as expected from an ionosphere that produces two distinct reflections. An oversimplified but instructive model of this process is as follows. Let there be two ionospheric reflection altitudes h_1 and h_2, with $h_2 > h_1$. The region between the reflection altitudes has an index

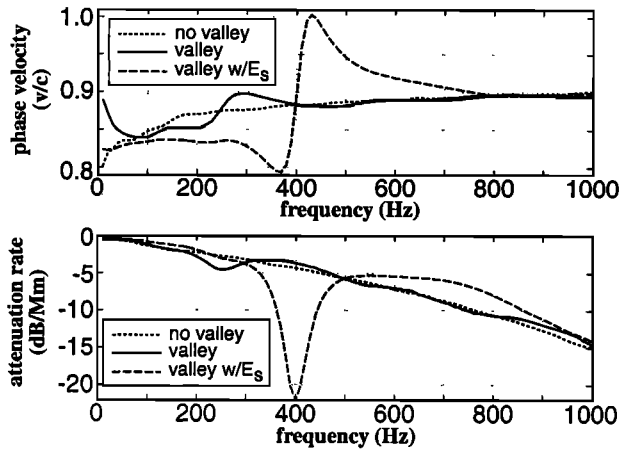

Figure 4. QTEM mode characteristics (phase velocity and attenuation rate) computed with LWPC for the three profiles in Figure 2. The differences demonstrate the importance of the E region on ELF propagation.

of refraction $n_h \gg 1$, and the region below h_1 is free space. For any angle of incidence below h_1 the refracted wave above h_1 will have a nearly vertical wave normal angle because $n_h \gg 1$. Thus the phase difference between the two reflected waves in the free space region is $\phi_h = \omega n_h(h_2 - h_1)/c$, where c is the speed of light. The two waves will interfere destructively if $\phi_h = (2m-1)\pi$ and constructively if $\phi_h = 2m\pi$. The nearly constant spacing between adjacent minima and maxima ($\Delta f \approx 110$) implies that $n_h(h_2 - h_1) = c/(2\Delta f) = 1360$ km. Reasonable E region valley parameters ($N_e = 500\,\mathrm{cm}^{-3}$, $\nu = 6000\,\mathrm{s}^{-1}$, and $f_b = 1.5$ MHz) give an X-mode index of refraction of ~20 at 500 Hz, giving $h_2 - h_1 \approx 68$ km. This simple estimate is quite close to the height difference between the underside of the D region (~80 km) and the top of the E region valley (~160 km), suggesting that the double-reflection process is responsible for the subionospheric ELF attenuation rate and phase velocity variations. The process is similar with an E_s layer that generates an even stronger secondary reflection and resonance.

The above simulations show that E_s and ambient variations affect nighttime subionospheric ELF propagation. On the basis of the simplified multiple reflection analysis, the observable quantities that contain information about the E region are the frequencies and depth of the amplitude minima and maxima. We explore how these quantities depend on quantitative E region characteristics and whether these characteristics can be extracted from measurements of subionospheric broadband ELF radiation from lightning discharges. For the remainder of the paper we focus primarily on non-E_s ionospheres.

4. Quantitative E Region Remote Sensing

ELF propagation dependence on the E region ionosphere opens the possibility of remotely sensing the electron density in this region. As discussed in section 1, the value of this ELF technique is that it is sensitive to E region valley parameters that are difficult to measure by other techniques. However, we need to quantitatively understand this sensitivity in order to probe this region with ELF.

A broadband ELF source is ideal for this application because the resonances can be easily detected with a complete ELF spectrum. Nature has provided us with such a source in lightning discharges. We use the LWPC model to simulate, for a variety of ionospheres, the ELF spectra of the signal radiated by a lightning discharge and received 2000 km away. We assume that the lightning discharge is an impulsive source for frequencies up to 1 kHz, a valid assumption since the risetimes and fall times of lightning current are usually less than a few hundred microseconds. Every lightning discharge generates quasi-static electric fields in the mesosphere that drive slowly varying relaxation electric currents that generate their own electromagnetic fields [*Greifinger and Greifinger*, 1976]. These relaxation-driven fields, which are not implicitly calculated by mode theory simulations, can be significant and therefore can affect our assumption of an impulsive source. Recent simulations have shown, how-

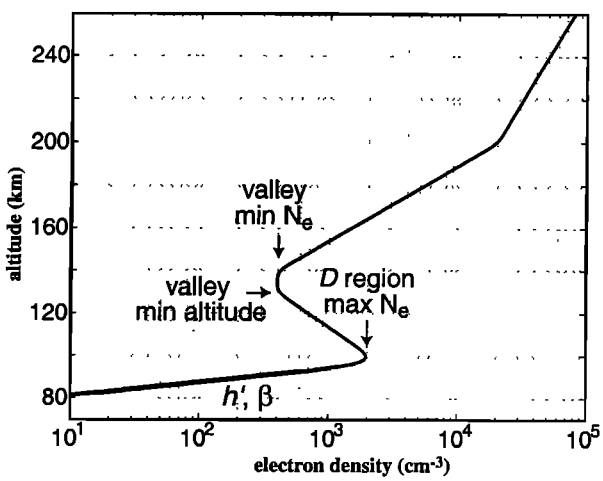

Figure 5. Five-parameter ionospheric model used to calculate the sensitivity of ELF propagation to ionospheric variability.

ever, that these relaxation-driven fields are insignificant 700 km from the source above 50 Hz [*Cummer*, 2000]. Thus, for our propagation distances (>1000 km) and frequencies (>50 Hz), the lightning source can be treated as impulsive. Further details on modeling ELF radiation from lightning are given by *Cummer and Inan* [2000].

Figure 5 shows a five-parameter ionosphere which is a slightly smoothed piecewise exponential electron density profile that we use to quantitatively investigate the effects of ionospheric changes on the ELF spectrum. The parameters H_{val}, E_{min}, and D_{max} describe the height of the E region valley, the minimum N_e in the valley, and the peak D region electron density below the valley, respectively. The D region parameters h' and β are the altitude and inverse scale height of an exponentially increasing model electron density profile originally described by *Wait and Spies* [1964] and commonly used in D region modeling. The D region electron density profile is given by $N_e(h) = 1.43\times10^{7}\exp(-0.15h')\exp\left[(\beta-0.15)(h-h')\right]\mathrm{cm}^{-3}$. We simulate the effect of perturbations from a basic nighttime ionosphere ($h' = 85$ km, $\beta = 0.5\ \mathrm{km}^{-1}$, $H_{\mathrm{val}} = 130$ km, $E_{\mathrm{min}} = 400\ \mathrm{cm}^{-3}$, and $D_{\mathrm{max}} = 2000\ \mathrm{cm}^{-3}$) in all parameters individually to understand which might be measurable from broadband ELF spectra.

Figure 6 shows the effect of variations in the five ionospheric parameters described above on the broadband ELF spectrum observed 2000 km away from the lightning discharge (or any impulsive source). The top panel shows that reducing E_{min} increases both the frequency and depth of the ELF resonances. This is precisely what is predicted by the approximate analysis in section 3. Decreasing E_{min} reduces the average index of refraction n_h between the two reflecting layers, which increases the resonance frequencies. Decreasing E_{min} also reduces the attenuation of the fields which penetrate the first reflecting altitude and reach the second reflecting altitude, which increases the amplitude of the second reflection and therefore leads to deeper interference minima and maxima.

The middle three panels of Figure 6 show that variations in D_{max}, H_{val}, and h' all have very similar effects on the ELF spectrum. Increasing H_{val}, increasing D_{max}, and decreasing h' all reduce the resonant ELF frequencies without changing the resonance sharpness. All of these effects are predicted by the approximate analysis in section 3. Decreasing h' reduces the first reflection altitude h_1, and increasing H_{val} increases the second reflection altitude h_2, which in both cases increases the reflection altitude difference $\Delta h = h_2 - h_1$ and therefore reduces the resonance frequencies. Increasing D_{max} effectively

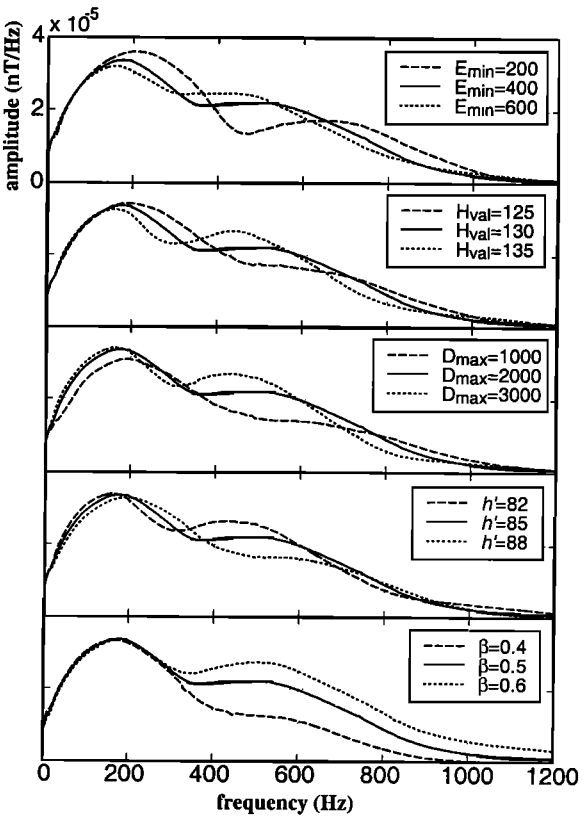

Figure 6. Variation in ELF spectrum with the ionospheric parameters in Figure 5.

increases the index of refraction n_h between the two reflection altitudes, which reduces the resonance frequencies just as does increasing Δh. The D region altitude h' can be inferred independently using VLF lightning propagation measurements [*Cummer et al.*, 1998], but the similarity of the effects of H_{val} and D_{max} on ELF propagation makes it difficult to measure both with this method.

The last panel of Figure 6 shows that the D region inverse scale height β does not change the resonance frequencies, but does strongly affect ELF attenuation above ~300 Hz. The D region inverse scale height β can also be measured from VLF observations [*Cummer et al.*, 1998], but the strong ELF dependence provides an independent and perhaps more sensitive measurement of this parameter.

Given how ionospheric parameters affect the ELF spectrum, the following procedure may be used to determine the probable ionosphere given an ELF spectrum. Assuming that h' is already known from the broadband VLF spectrum [*Cummer et al.*, 1998], select E_{min} to match

the depth of the observed resonances, select either D_{max} or H_{val} to match the resonance frequencies, and select β as needed to match the upper ELF (500–1500 Hz) field amplitude. There is inherent nonuniqueness in the deduced ionosphere because of the similarity D_{max} and H_{val}. This result is not surprising, since we are only matching a three-parameter measurement (resonance frequency, resonance depth, and upper ELF amplitude) to a four-parameter model. To resolve this, in section 5, we fix $D_{max} = 2000$ cm^{-3} and only vary H_{val} to match the observations.

5. Comparison of Observations and Simulations

Lightning-generated broadband ELF spectra do show significant variability that can be attributed to ionospheric E region variations. We use nighttime horizontal magnetic field measurements recorded by the Stanford University ELF-VLF Radiometer Experiment [*Chrissan and Fraser-Smith*, 1996] in July 1996. Using a procedure essentially identical to that of *Cummer et al.* [1998], we temporally average transient radio atmospherics (sferics) launched by lightning discharges in a small geographic region (as measured by the National Lightning Detection Network [*Cummins et al.*, 1998]) in a 30 min time period, which is usually long enough to accumulate enough sferics for a good signal-to-noise ratio. We implicitly assume that the ionosphere does not vary significantly over this period, and we do not include waveforms from large positive discharges that tend to have significant continuing currents [*Uman*, 1987, p. 200] and are therefore not an impulsive ELF source. The ELF portion of the spectrum of the resulting average waveform, which includes the effect of a single-pole, high-pass filter at 420 Hz in the receiver, is the measured ELF spectrum.

The solid lines in Figure 7a are measured ELF spectra from July 22 (0700–0730 UT), July 24 (0400–0430 UT), and July 26 (0400–0430 UT and 0845–0915 UT). The propagation distance from source to receiver for these spectra is ~2000 km. The mean amplitudes differ slightly between periods because the average lightning discharge strength is different in each period. The details of the spectra, including the resonance frequencies, vary more than could be caused by just the simultaneous D region variations measured using the technique of *Cummer et al.* [1998], which we applied to the simultaneous VLF data. This indicates significant E region changes between the four periods. For the first three time periods the dashed lines in Figure 7a are model ELF spectra found by using the iterative matching procedure described in section 4. The generally good agreement between the simulations and observations means that the inferred ionospheres do explain the observations, subject to the nonuniqueness issues discussed in section 4. The ELF spectrum of the last time period could not be reproduced with any reasonable variation of the ionospheric parameterization in Figure 5,

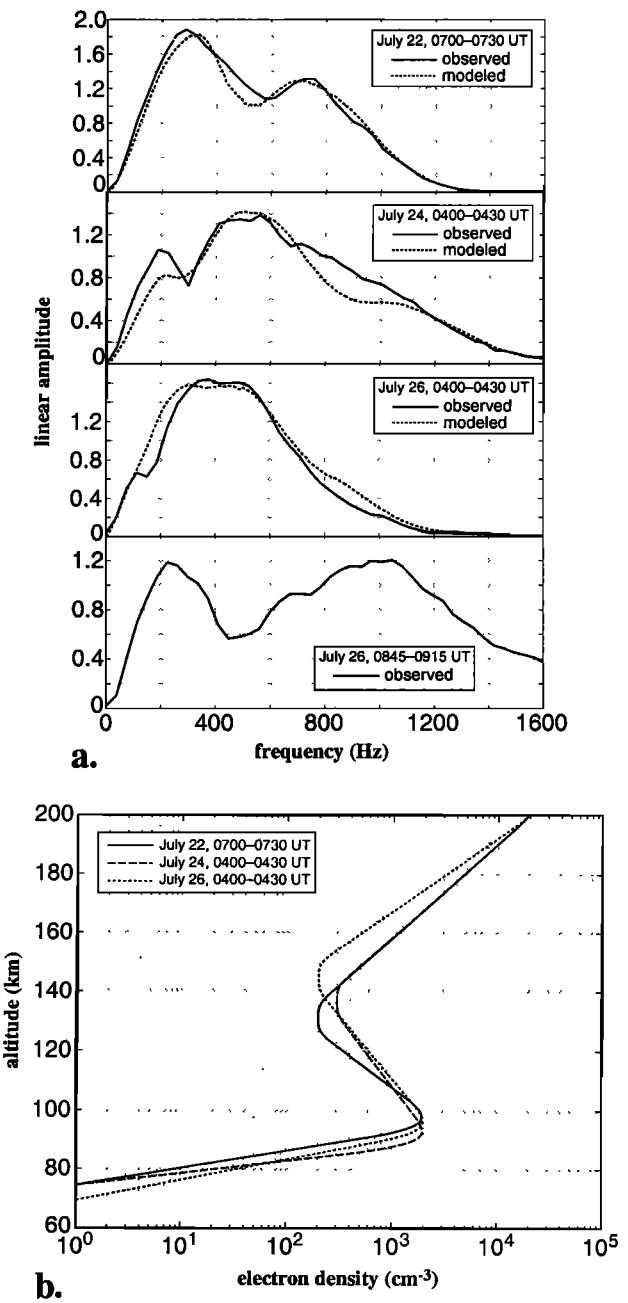

Figure 7. (a) Observed broadband ELF spectra and, in three cases, model ELF spectra that agree well. (b) The three ionospheres inferred from the observations.

and it does not have an unusually sharp resonance indicative of an E_s layer. Clearly, the nighttime E region can be highly variable, and matching all of the data requires a broader ionospheric parameterization.

Figure 7b shows the three D and E region electron density profiles that reproduced the observations in the first three time periods. The ionospheric variability is significant but not extraordinary, highlighting the sensitivity of ELF spectra to the D and E region ionosphere. Though none of the observed spectra contained evidence of E_s, the theoretically high sensitivity shown in section 3 should make E_s layers easily detectable with this technique.

It should be mentioned that the values of β extracted from the VLF technique of *Cummer et al.* [1998] and the ELF technique described here, both of which assume a single scale height below ~90 km, differ by as much as 0.15 km^{-1}. The actual D region ionosphere may have multiple scale heights and may, for example, contain a sharp ledge as does the profile of *Hale* [1994]. The ELF and VLF techniques are probably sensitive to the scale height for different altitude ranges, which may explain this discrepancy.

6. Summary and Conclusions

Although the ionospheric reflection altitude of electromagnetic waves generally decreases with decreasing frequency, lower losses and sharper gradients in the index of refraction can generate E-F region reflections at ELF that do not occur for VLF. This high-altitude reflection makes subionospheric ELF propagation depend on details of the ionospheric E region and thereby provides a technique for remotely sensing this region. Using the full wave LWPC model, we showed that signatures of both sporadic E and ordinary nighttime E region variability are present in broadband spectra of subionospherically propagated ELF waves. Resonances from the interference of multiple ionospheric reflections create amplitude minima and maxima whose frequency and depth are controlled by different parameters of a five-parameter model ionosphere. Three of these parameters produce very similar effects in the simulated ELF spectra (one of which can be measured independently), leaving three parameters that can be measured effectively with this technique.

To demonstrate the technique, we analyzed measured ELF spectra produced by lightning discharges, a natural broadband ELF source, on a 2000 km source-receiver path on 3 different days in 1996. Averaging multiple sferics to generate clean broadband ELF spectra, we used iterative simulations to find the ionospheres that fit the observations. In general, the agreement was good, and we found that in most cases the variations in the spectra could be explained by normal E region variability.

The utility of the single propagation path technique that we have demonstrated can be extended significantly with multiple receivers and multiple source locations. Since only a single mode propagates in the frequency range of interest, a WKB-type solution is valid in the presence of even relatively sharp (with respect to wavelength) horizontal ionospheric inhomogeneities. Thus the observed ELF spectrum is essentially that which would be produced by a homogeneous ionosphere that is the mean ionosphere along the entire path. With multiple receivers and source locations, such path-integrated measurements can be inverted using tomographic techniques to deduce the two-dimensional horizontal structure of the ionosphere. Such a technique would be especially useful in tracking the size and motion of large inhomogeneities like sporadic E.

References

Bannister, P. R., Variations in extremely low frequency propagation parameters, *J. Atmos. Terr. Phys.*, *37*, 1203–1210, 1975.

Barr, R., The effect of sporadic-E on the nocturnal propagation of ELF radio waves, *J. Atmos. Terr. Phys.*, *39*, 1379–1387, 1977.

Bilitza, D., International Reference Ionosphere—Status 1995/96, *Adv. Space Res.*, *20(9)*, 1751–1754, 1997.

Budden, K. G., *The Propagation of Radio Waves*, Cambridge Univ. Press, New York, 1985.

Chrissan, D. A., and A. C. Fraser-Smith, Seasonal variations of globally measured ELF/VLF radio noise, *Radio Sci.*, *31*, 1141–1152, 1996.

Cummer, S. A., Modeling electromagnetic propagation in the Earth-ionosphere waveguide, *IEEE Trans. Antennas Propag.*, *in press*, 2000.

Cummer, S. A., and U. S. Inan, Modeling ELF radio atmospheric propagation and extracting lightning currents from ELF observations, *Radio Sci.*, *35*, 385–394, 2000.

Cummer, S. A., U. S. Inan, and T. F. Bell, Ionospheric D region remote sensing using VLF radio atmospherics, *Radio Sci.*, *33*, 1781–1792, 1998.

Cummins, K. L., E. P. Krider, and M. D. Malone, The US National Lightning Detection Network and applications of cloud-to-ground lightning data by electric power utilities, *IEEE Trans. Electromagn. Compat.*, *40*, 465–480, 1998.

Greifinger, C., and P. Greifinger, Transient ULF electric and magnetic fields following a lightning discharge, *J. Geophys. Res.*, *81*, 2237–2247, 1976.

Hale, L. C., Coupling of ELF/ULF energy from lightning and MeV particles to the middle atmosphere, ionosphere, and global circuit, *J. Geophys. Res.*, *99*, 21,089–21,096, 1994.

Hughes, H. G., and R. J. Gellenberger, Propagation of extremely low-frequency (ELF) atmospherics over a mixed day-night path, *J. Atmos. Terr. Phys.*, *36*, 1643–1661, 1974.

Johnson, M. P., U. S. Inan, S. J. Lev-Tov, and T. F. Bell, Scat-

tering pattern of lightning-induced ionospheric disturbances associated with early/fast VLF events, *Geophys. Res. Lett.*, *26*, 2363–2366, 1999.

Mechtly, E. A., S. A. Bowhill, L. G. Smith, and H. W. Knoebel, Lower ionosphere electron concentration and collision frequency from rocket measurements of Faraday rotation, differential absorption, and probe current, *J. Geophys. Res.*, *72*, 5239–5245, 1967.

Morfitt, D. G., and C. H. Shellman, MODESRCH, an improved computer program for obtaining ELF/VLF/LF mode constants in an Earth-ionosphere waveguide, *Interim Rep. 77T*, Nav. Electr. Lab. Cent., San Diego, Calif., 1976.

Pappert, R. A., and J. A. Ferguson, VLF/LF mode conversion model calculations for air to air transmission in the earth-ionosphere waveguide, *Radio Sci.*, *21*, 551–558, 1986.

Pappert, R. A., and W. F. Moler, Propagation theory and calculations at lower extremely low frequencies (ELF), *IEEE Trans. Commun.*, *22*, 438–451, 1974.

Pappert, R. A., and W. F. Moler, A theoretical study of ELF normal mode reflection and absorption produced by nighttime ionospheres, *J. Atmos. Terr. Phys.*, *40*, 1031–1045, 1978.

Ratcliffe, J. A., *The Magneto-Ionic Theory*, Cambridge Univ. Press, New York, 1959.

Rishbeth, H., and O. K. Garriott, *Introduction to Ionospheric Physics*, Academic, San Diego, Calif., 1969.

Sechrist, C. F., Jr., Comparisons of techniques for measurement of D-region electron densities, *Radio Sci.*, *9*, 137–149, 1974.

Uman, M. A., *The Lightning Discharge*, Academic, San Diego, Calif., 1987.

Wait, J. R., and K. P. Spies, Characteristics of the Earth-ionosphere waveguide for VLF radio waves, *NBS Tech. Note 300*, 1964.

Watt, A. D., *VLF Radio Engineering*, Pergamon, Tarrytown, N. Y., 1967.

S. A. Cummer, Electrical and Computer Engineering Department, Duke University, Durham, NC 27708. (cummer@ee.duke.edu)

U. S. Inan, STAR Laboratory, Stanford University, Durand 324, Stanford, CA 94305-9515.

(Received February 12, 2000; revised August 23, 2000; accepted August 24, 2000.)